Journal of Materials Science and Engineering A 10 (1-2) (2020) 30-36
doi: 10.17265/2161-6213/2020.1-2.004

Effect of Photoanode Modification on Charge Transport, Recombination and Efficiency of Dye Sensitized Solar Cells Using Synthetic Organic Dyes

Me Me Theint[1], Hnin Ei Maung[2], Su Htike Aung[1], Nyein Wint Lwin[1] and Than Zaw Oo[3]

1. Department of Physics, University of Mandalay, Mandalay 05032, Myanmar

2. Department of Physics, Mandalar Degree College, Mandalay 05061, Myanmar

3. Universities' Research Centre, University of Yangon, Yangon 11041, Myanmar

Abstract: The DSSCs (Dye-sensitized solar cells) with photoanode using different sizes of particulate TiO_2 (18 nm, 30 nm and 200 nm) have been fabricated. The synthetic organic dyes (LEG4) was used as photosensitizer. The present work mainly investigates the influence of TiO_2 photoanode modification on light absorption, charge transport and carrier recombination which are then correlated to the device efficiency measured under AM1.5 solar irradiance. The DSSCs with photoanode using larger 200-nm-TiO_2 as light scatterer outperform other devices without larger TiO_2. It is attributed to an increase in harvesting photons (by UV-vis spectroscopic measurement) via light scattering, smaller ideality factor (by dark current analysis), thus lower recombination possibility, lower charge transfer resistance and longer electron lifetime (by electrochemical impedance spectroscopy) which results in longer electron diffusion and higher charge collection efficiency. The photoanode modification in DSSCs has a strong impact on optical and charge transport properties, and eventually on the photovoltaic performance.

Keywords: DSSCs, LEG4 dye, TiO_2 photoanode, charge transport, recombination.

1. Introduction

The DSSC (dye-sensitized solar cell) is a photo electrochemical solar cell using redox mediator to transport electrons and become an attractive alternative to the widely used Si-based solar cell due to its low processing cost, ease of fabrication, moderate efficiency [1-4]. In order to improve power conversion efficiency of DSSCs, many attempt shave been devoted to modification of the DSSC components such as photoanode, electrolyte, photosensitizer dye molecules and counter electrode [5]. Among them, the photoanode modification is of crucial importance in enhancing device efficiency since it works as both photon harvestor (by photosensitizer dye) as well as charge transporter (by n-type semiconductor) [6-8].

Corresponding author: Than Zaw Oo, Ph.D., professor, research fields: materials science and engineering.

Mesoporous nanoparticulate TiO_2 semiconductor is a commonly used photoanode material for its relatively high energy conversion efficiency, high specific surface area [9], non-toxicity and low cost [10]. However one major constraint of this material is its random electron transport which would lead to charge carrier recombination in the device [11]. In addition, due to its small size, it is transparent to visible light, weak in visible light scattering and high recombination of photo generated electron-hole pairs [12]. The charge recombination, the electron loss in the device, is one of the principal factors limiting power conversion efficiency [13].

To address the charge recombination issue and achieve good scattering performance, several strategies have been utilized over the years. For instance, integration of photonic crystals and larger sized metal oxide nanostructures at photoanode which increases the absorption path-length of photons via

light scattering [14], integration of plasmonic metal nanostructures in TiO_2 which offer light concentration and better light scattering via a phenomenon of surface plasmonics, and doping of metal or non-metal into TiO_2 which would change the sub-band states, modulating the band gap [15, 16]. Many attempts on photoanode modification in DSSCs and associated efficiency improvements are widely acknowledged [17, 18]. The rationales of efficiency enhancement via modifying the photoanode using different sizes of particulate TiO_2 in terms of current leakage, charge transport and carrier recombination have not yet widely been explored. In the present work, the photoanodes of DSSCs were fabricated using different sizes of particulate TiO_2 so as to study the effect of modifying photoanode on light absorption, current leakage, charge transport and charge recombination resistance, eventually on the device efficiency.

2. Experimental Section

The FTO (fluorine doped tin oxide) coated glass substrates were ultrasonically cleaned with detergent, alcohol and deionized water followed by nitrogen blow and UV exposure for 15 min to ensure full dryness and remove organic contamination on the substrate. The mesoporous TiO_2 films were screen-printed on FTO substrates using TiO_2 paste (Dyesol DSL 30 NRD-T) with different nanoparticle sizes of 18 nm, 30 nm and 200 nm. We prepared six different multilayer TiO_2 samples, namely (i) 18 nm, (ii) 18/18 nm, (iii) 18/200 nm, (iv)30 nm, (v) 30/30 nm and (vi) 30/200 nm. The resulting TiO_2 films were immersed in the solution of organic dye[3-{6-{4-[bis(2',4'dibutyloxybiphenyl-4yl)amino]phenyl}-4,4-dihexylcyclopenta[2,1b:3,4b']dithiophen-2-yl}-2-cyanoacrylic acid, in short, LEG4 (DyenamoDN-F05)] for 24 hours in order to infiltrate dye into TiO_2 matrices. They were then rinsed with ethanol to remove unwanted solid residues. The thickness of TiO_2 layers was measured by surface profilometer (Tencor, Alpha-Step IQ).

The absorption spectra of dye loaded TiO_2 films were recorded using UV-Vis spectrophotometer (Thermo Scientific, Genesys 10S) in the wavelength range of 300-900 nm. The dye sensitized solar cells (DSSCs) were assembled by introducing the redox electrolyte (0.05 M/I_2 and 0.5 M/LiI in acetonitrile) between the dye loaded TiO_2 electrode (photoanode) and platinum counter electrode. The current–voltage (I-V) characteristics of DSSCs were measured at room temperature by using a source meter (Keithley 2400) and solar simulator (Newport/Oriel). The AM 1.5 illumination of intensity 1000 W/m^2 was calibrated using a standard Si solar cell certified by NREL (National Renewable Energy Laboratory). The I-V characteristics were also recorded in dark for extraction of ideality factor. EIS (Electrochemical impedance spectroscopic) measurement was also performed in dark to analyze the charge transport resistance and recombination lifetime in the DSSCs using the potentiostat/Galvanostat electrochemical analyzer (Corrtest: CS350). The impedance spectra were analyzed using the Z view software. The frequency range is 0.01-100 kHz and the magnitude of AC signal is 10 mV.

3. Results and Discussion

First, we studied the optical absorption of LEG4 dye loaded on different TiO_2 scaffolds [18 nm (4 μm), 18/18 nm (7 μm), 18/200 nm (9 μm), 30 nm (4 μm), 30/30 nm (7 μm) and 30/200 nm (9 μm)]. The values in the parenthesis represent the thickness of TiO_2 films. Their optical absorption spectra are shown in Fig. 1. For all samples, the absorption peak is centered at 475 nm which is the characteristic of LEG4 [19]. It is observed that the optical absorption increases with increasing TiO_2 layer thickness which is attributed to increased dye surface area (higher dye loading) with thicker TiO_2 [20]. The absorption enhancement is more pronounced in the 18/200 nm and 30/200 nm samples which is ascribed to the back light scattering by larger TiO_2 nanoparticles (200 nm) thereby

increasing the path length of photons [21].

Next, we used the LEG4 dye/TiO_2 as photoanode in DSSCs and studied the effect of photoanode modification on the power conversion efficiency of DSSCs. Fig. 2 shows the I-V characteristics of DSSCs with six different TiO_2 photoanodes under AM 1.5 solar irradiance. The photovoltaic device parameters extracted from the *I-V* curves are listed in Table 1. In the DSSCs with 18-nm-based TiO_2, higher efficiency (η) of 3.19% with open circuit voltage (V_{oc}) of 0.68 V, short circuit current density (J_{sc}) of 6.26 mA/cm^2 and fill factor (FF) of 0.52 was realized with 18/200 nm TiO_2 photoanode. Likewise, in the DSSCs with 30-nm-based TiO_2, higher η of 4.76% with V_{oc} = 0.73 V, J_{sc} = 8.49 mA/cm^2 and *FF* = 0.61 was realized with 30/200 nm TiO_2 photoanode. Higher efficiency with 18/200 nm and 30/200 nm TiO_2 photoanode is contributed from higher values of all device parameters (V_{oc}, J_{sc} and *FF*) with major contribution from J_{sc} enhancement. This photocurrent enhancement would be due to an effective back scattering of light by larger TiO_2 nanoparticles (200 nm), which effectively increased dye absorption [22] evidenced by the absorption spectra (Fig. 1). The light scattering at TiO_2 scaffolds is thus an important phenomenon influencing the performance of DSSCs. It is also found that further increase in thickness of 200-nm-TiO_2 negated the efficiency of devices (the data is not shown here).

Following the determination of device efficiency, charge recombination and leakage current in DSSCs upon modifying the photoanode were also investigated

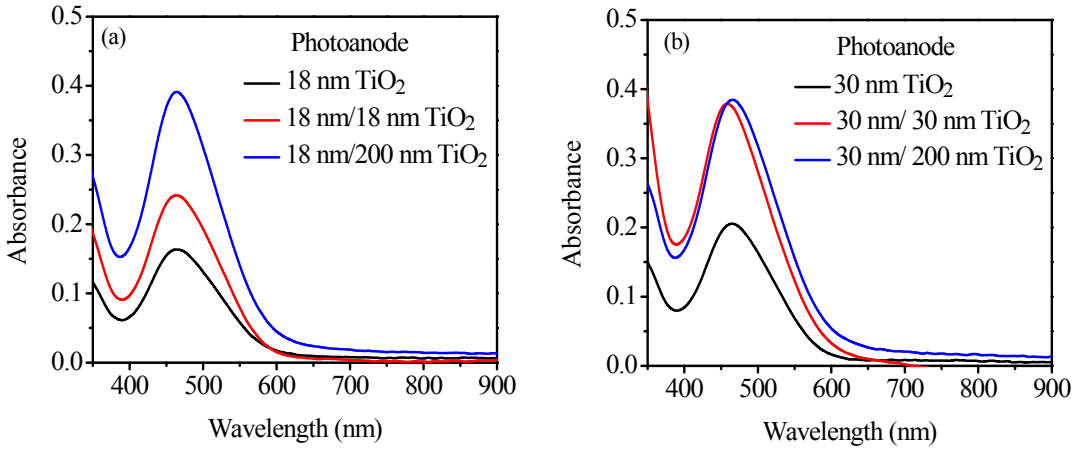

Fig. 1 The absorption spectra of the LEG4 dye loaded on different TiO_2 scaffolds

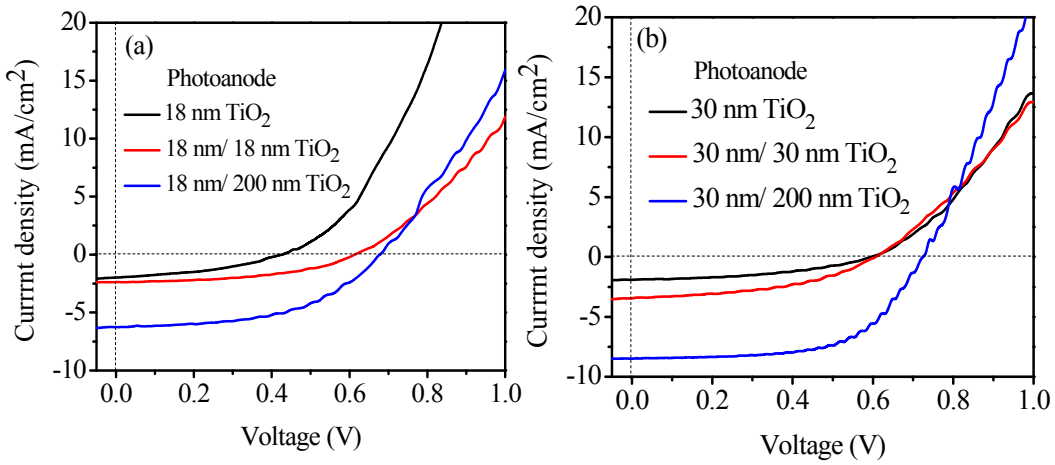

Fig. 2 The J-V characteristics for DSSCs using different TiO_2 photoanodes.

Table 1 Device parameters (V_{oc}, J_{sc}, FF, η) of DSSCs using different TiO_2 photoanodes.

TiO_2 Photoanode	V_{oc} (V)	J_{sc} (mA/cm^2)	FF (%)	η (%)
18 nm	0.424	1.983	38.787	0.408
18 nm/18 nm	0.611	2.370	48.393	1.045
18 nm/200 nm	0.678	6.263	52.668	3.194
30 nm	0.590	1.909	44.158	0.742
30 nm/30nm	0.605	3.446	46.199	1.377
30 nm/200 nm	0.728	8.498	61.605	4.762

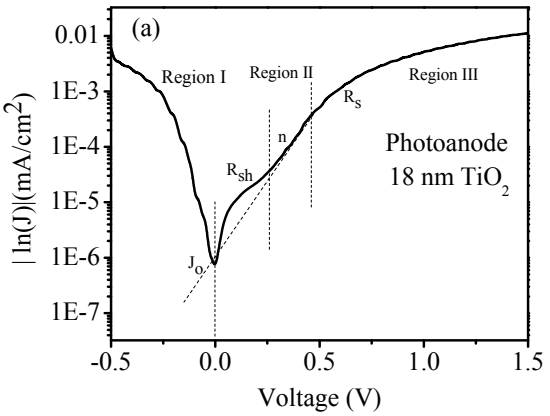

Fig. 3 The ln(J)-V characteristics in dark of DSSCs with 18 nm TiO_2 photoanode.

using dark current analysis. The informative parameters such as ideality factor (n), reverse saturation current (J_o), series resistance (R_s) and shunt resistance (R_{sh}) were extracted from the dark J-V curve. The device can be simply described by a one-diode equivalent model and the current flow across the device is represented by the general diode equation taking into account the series and shunt resistances.

$$J = J_O\left[\exp\left(\frac{q(V - JAR_S)}{nkT}\right) - 1\right] + \frac{V - JAR_S}{AR_{sh}} - J_{ph}$$

where, J_o is the reverse saturation current density, q is the electronic charge, V is the applied voltage, A is the effective diode area, n is the ideality factor, k is the Boltzmann constant, T is the absolute temperature, R_s is the series resistance and R_{sh} is the shunt resistance. In dark, the photocurrent density (J_{ph}) is zero. Fig. 3 reveals the ln(J)-V characteristics in dark of DSSCs with 18 nm TiO_2. In the plot [ln(J) vs. V], the three regions can be identified. Region I is a linear region at reverse voltages and low forward voltages where current is limited by shunt resistance R_{sh} (leakage current). Region II exhibits an exponential behavior at immediate forward voltages where current is controlled by a diode. Region III is a linear region at high forward voltages where the current is limited by series resistance R_s. Obviously, the R_s and R_{sh} can be extracted from the region I and III respectively. The slope and the extrapolated-to-zero-volt point of region II gives the ideality factor (n) and J_o respectively [23]. The extracted parameters are listed in Table 2.

The ideality factor (n) reflects the quality of interfaces within device and recombination behaviors at that interfaces. Enhanced disorder or defects induced recombination loss typically results in higher n values, deviating from the ideal diode behavior [24] The n value is 3.0 and 2.6 in the DSSC with 18 nm and 30 nm TiO_2 photoanode respectively. Upon modifying the photoanode with larger TiO_2 (200 nm), the n decreased to 1.7 and 1.3 respectively in the DSSCs with 18/200 nm and 30/200 nm photoanode. It is indicative of reduced charge recombination and consequently the V_{oc} increased in these devices [25]. The reverse saturation current density (J_o) is a leakage current flowing across the charge collecting electrodes in the device. As seen in Table 2, decreased J_o with larger TiO_2 suggests less current leakage in these devices. Also observed are the lower R_s and higher R_{sh} in DSSCs with larger TiO_2 which would result in higher FF in these devices.

Electrochemical impedance spectroscopy (EIS) is one of the most important tools to elucidate the charge transfer and transport processes in various electrochemical systems including DSSCs. Fig. 4 (a, c)

depicts the Nyqu ist plots of EIS spectra with the inset showing the schematic of the internal resistance related to the charge transfer kinetics in DSSCs. There are two semicircles in EIS spectra; the small one at high frequency fitted to a charge transfer resistance (R_{ct1}) and chemical capacitance (C_1) is assigned to electrochemical reaction at the redox electrolyte/platinum interface while the larger one at low frequency fitted to a charge transfer resistance (R_{ct2}) and chemical capacitance (C_2) is assigned to

Table 2 Dark current analysis parameters (n, J_o, R_s and R_{sh}).

TiO_2 Photoanode	n	J_o (mA/cm^2)	R_s (kΩcm^2)	R_{sh} (kΩcm^2)
18 nm	3.0	9.74×10^{-7}	0.090	7.773
18 nm/18nm	2.8	5.73×10^{-7}	0.052	33.155
18 nm/200 nm	1.7	2.16×10^{-7}	0.048	55.822
30 nm	2.6	8.31×10^{-7}	0.056	16.591
30 nm/30nm	2.2	7.95×10^{-7}	0.050	33.775
30 nm/200 nm	1.3	1.65×10^{-7}	0.038	37.085

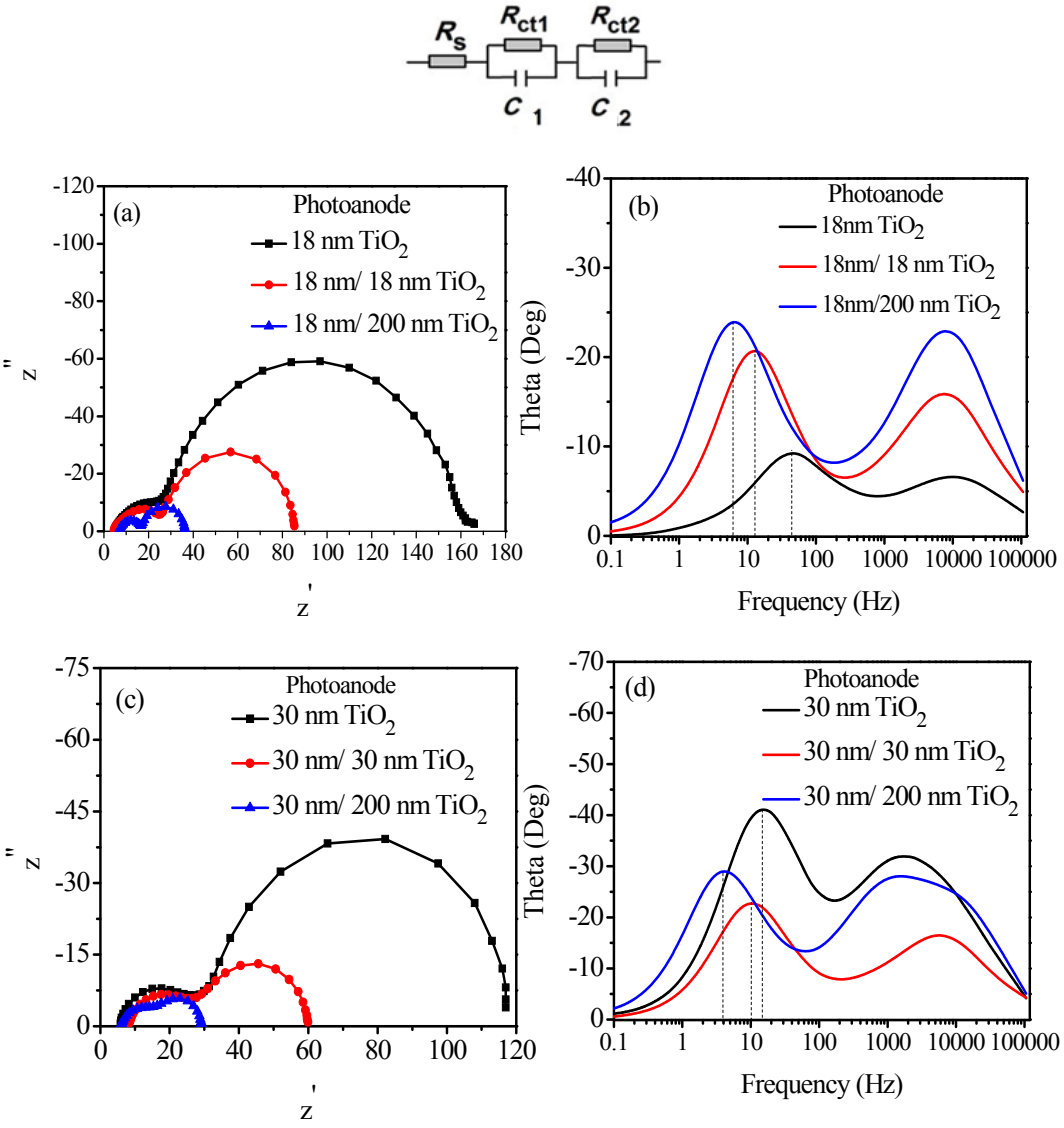

Fig. 4 EIS spectra (a, c) Nyquist plot and (b, d) Bode plots for DSSCs with different photoanodes The schematic above the Fig depicts the internal resistance related to the charge transfer kinetics in DSSC).

Table 3 EIS data of DSSCs with different TiO_2 photoanodes.

TiO_2 Photoanode	$R_{ct1}(\Omega)$	$R_{ct2}(\Omega)$	F_{max}(Hz)	τ_e (ms)
18 nm	21.7	139.4	46.6	3.4
18 nm/18 nm	20.9	60.7	12.4	12.7
18 nm/200 nm	9.9	19.6	6.5	24.2
30 nm	23.2	88.8	15.3	10.4
30 nm/30 nm	18.2	33.3	9.8	16.2
30 nm/200 nm	9.0	14.2	4.0	39.7

charge transfer reactions at the TiO_2/dye/electrolyte interface and the accumulation/transport of the injected electrons within TiO_2 film. The total impedance of the DSSC is the sum of the impedance at the Pt and TiO_2 electrodes, and the impedance due to diffusion of tri-iodide in the electrolyte. These data were analyzed with a non-linear least square fitting program using Z view software.

The resulting impedance parameters listed in Table 3 show that the DSSCs with TiO_2 scattering layer (18 nm/200 nm and 30 nm/200 nm) exhibits the lower values of R_{ct1} and R_{ct2} which indicates the more efficient charge transfer process at the interfaces of electrolyte/Pt and TiO_2/dye/electrolyte. The Bode phase plots of EIS spectra (Fig. 4b, d) display the characteristic frequency peaks of the charge transfer process at different interfaces which are listed in Table 3. The characteristic frequency (f) is related to the inverse of electron lifetime (τ_e) [$\tau_e = 1/(2\pi f_{max})$ where, f_{max} is the maximum frequency of the mid-frequency peak]. The electron lifetimes are longer with TiO_2 scattering layer, 24.2 ms with 18 nm/200 nm photoanode and 39.7 ms with 30 nm/200 nm photoanode. Longer electron lifetime could favor the electron transport through a longer distance which lowers the recombination resistance (R_{rec}) in the device [26].

4. Conclusions

The DSSCs with a multilayer structure of TiO_2 using different nanoparticle sizes (18 nm, 30 nm and 200 nm) as photoanode were fabricated and characterized. It was found that the DSSCs with larger TiO_2 (200 nm) as scattering layer rendered a relatively higher device efficiency which is correlated to the optical and charge transport properties and charge recombination in the device. Optical absorption enhancement with TiO_2 scattering layer is due to increased dye loading in the TiO_2 and back light scattering by larger TiO_2 particles. Dark current analysis revealed that ideality factor and reverse saturation current are lower with TiO_2 scattering layer which indicate the low current leakage and charge recombination probability. Electrochemical impedance spectroscopy measurement indicated the lower charge transfer resistance suggesting high recombination resistance and longer electron lifetime which would result in higher charge collection and photocurrent generation in the device. To sum up, relatively higher device efficiency with photoanode using layer TiO_2 as scattering layer is attributed to increased light absorption, favorable charge transport and lower charge recombination in the device. The photoanode modification is critical in modulating the optical and charge transport properties and photovoltaic performance of DSSCs.

Acknowledgments

Authors acknowledge the project grant (Activity code: MYA-01, 2017-2019) from International Science Program (ISP), Uppsala University, Sweden.

References

[1] Dang, C., Labie, R., Simoen, E., and Poortmans, J. 2018. "Detailed Structural and Electrical Characterization of Plated Crystalline Silicon Solar Cells." *Sol. Energ. Mater. Sol. Cells* 184: 57-66.

[2] Richhariya, G., et al. 2017. "Natural Dyes for Dye Sensitized Solar Cell: a Review." *Renew Sustain Energ.*

Rev. 69: 705-18.

[3] MAM, Al-A., et al. 2016. "Dye-sensitised Solar Cells: Development, Structure, Opera-tion Principles, Electron Kinetics, Characterisation, Synthesis Materials and Natural Photosensitisers." *Renew Sustain Energ. Rev.* 65: 183-213.

[4] Bhogaita, M., Shukla, A. D., and Nalini, R. P. 2016. "Recent Advances in Hybrid Solar Cells based on Natural Dye Extracts from Indian Plant Pigment as Sensitizers." *Sol. Energ.* 137: 212-24.

[5] Cai, H., Tanga, Q., Heb, B., Lia, R., and Yu, L. 2014. "Bifacial Dye−Sensitized Solar Cells with Enhanced Rear Efficiency and Power Output." *Nanoscale* 6: 15127-33.

[6] Yeoh, M. E., and Chan, K. Y. 2017. "Recent Advances in Photo-Anode for Dyesensitized Solar Cells: a Review." *Int. J. Energ. Res.* 41: 2446-67.

[7] Fan, K., Yu, J., and Ho, W. 2017. "Improving Photoanodes to Obtain Highly Efficient Dye-Sensitized Solar Cells: a Brief Review." *Mater. Horiz.* 4: 319-44.

[8] Ramanarayanan, R., Nijisha, P., Niveditha, C. V., and Sindhu, S. 2017. "Natural Dyes from Red Amaranth Leaves as Light-Harvesting Pigments for Dye-Sensitized Solar Cells." *Mater. Res. Bull.* 90: 156-61.

[9] Ganesh, R. S., Navaneethan, M., Ponnusamy S., et al. 2018. "Enhanced Photon Collection of High Surface Area Carbonate Doped Mesoporous TiO_2 Nanospheres in Dye Sensitized Solar Cells." *Mater. Res. Bull* 101: 353-62.

[10] Hosseinnezhad, M., Jafari, R., and Gharanjig, K. 2017. "Characterization of a Green and Environmentally Friendly Sensitizer for a Low Cost Dye-Sensitized Solar Cell." *Opto-Electron. Rev.* 25 (2): 93-8.

[11] Sarker, S., Seo, H. W., and Kim, D. M. 2013. "Electrochemical Impedance Spectroscopy of Dye-Sensitized Solar Cells with Thermally Degraded N719 Loaded TiO_2." *Chem. Phys. Lett.* 585: 193-7.

[12] Bisquert, J., Bertoluzzi, L., Mora-Sero, I., and Garcia-Belmonte, G. 2014. "Theory of Impedance and Capacitance Spectroscopy of Solar Cells with Dielectric Relaxation, Drift-Diffusion Transport, and Recombination." *J. Phys. Chem. C* 118 (33): 18983-91.

[13] Tang, X., Wang, Y., and Cao, G. 2013. "Effect of the Adsorbed Concentration of Dye on Charge Recombination in Dye-Sensitized Solar Cells." *J. Electroanal. Chem.* 694: 6-11.

[14] Naphade, R., Tathavadekar, M., Jog, J. P., Agarkar, S., and Ogale, S. 2014. "Plasmonic Light Harvesting of Dye Sensitized Solar Cells by Au-Nanoparticle Loaded TiO_2 Nanofibers." *J. Mater Chem. A* 2: 975-84.

[15] Mohamed, I. M. A., Dao, V. D., Barakat, N. A. M., Yasin, A. S., and Yousef, A. 2016. "Efficiency Enhancement of Dye-Sensitized Solar Cells by Use of ZrO_2- Doped TiO_2 Nanofibers Photoanode." *J. Colloid Interface Sci.* 476: 9-19.

[16] Amaral, R. C., Barbosa, D. R. M., Zanoni, K. P. S., and Iha, N. Y. M. 2017. "Natural Sensitizers for DSCs Improved with Nano-TiO_2 Compact Layer." *J. Photochem. Photobiol. Chem.* 346: 144-52.

[17] Calogero, G., Barichello, J., Citro, I., et al. 2018. "Photoelectrochemical and Spectrophotometric Studies on Dye-Sensitized Solar Cells (DSCs) and Stable Modules (DSCMs) based on Natural Apocarotenoids Pigments." *Dyes and Pigments* 155: 75-83.

[18] Sarker, S., Seo, H. W., and Kim, D. M. 2014. "Calculating Current Density-Voltage Curves of Dye-Sensitized Solar Cells: a Straightforward Approach." *J. Power Sources* 248: 739-44.

[19] Jiang, X., Marinado, T., Gabrielsson, E., Hagberg, D. P., Sun, L., and Hagfeldt, A. 2010. "Structural Modification of Organic Dyes for Efficient Coadsorbent-Free Dye-Sensitized Solar Cells." *J. Phys. Chem. C* 114 (6): 2799-805.

[20] Liang, M. S., Fong, Y. K., Khaw, C. C., and Liu, C. C. 2014. "Studies on the Effect of Crystallite Sizes and Scattering Layers on the Conversion Efficiency of Dye Sensitized Solar Cell." *J. Power Energy. Eng.* 2: 18-24.

[21] Yan, K., Qiu, Y., Chen, W., Zhang, M., and Yang, S. 2011. "A Double Layered Photoanode Made of Highly Crystalline TiO_2 Nanooctahedra and Agglutinated Mesoporous TiO_2 Microspheres for High Efficiency Dye Sensitized Solar Cells." *Energ. Environ. Sci.* 4: 2168-76.

[22] Yu, I. G., Kim, Y. J., Kim, H. J., Lee, C., and Lee, W. I. 2011. "Size Dependent Light-Scattering Effects of Nanoporous TiO_2 Spheres in Dye Sensitized Solar Cells." *J. Mater. Chem.* 21: 532-8.

[23] Usha, K., Mondal, B., Sengupta, D., Das, P., and Mukherjee, K. 2014. "Fabrication of Dye Sensitized Solar Cell Using Nanocrystalline TiO_2 and Optical Characterization of Photo-Anode." *Nanosci. and Nanoeng.* 2 (2): 29-35.

[24] Macabebe, E. Q. B., and Van Dyk, E. E. 2008. "Parameter Extraction from Dark Current-Voltage Characteristics of Solar Cells." *S. Afr. J. Sci.* 104 (9-10): 401-4.

[25] Ko, Y. S., Kim, M-H., and Kwon, Y-Uk. 2008. "Method to Increase the Surface Area of Titania Films and its Effects on the Performance of Dye Sensitized Solar Cells." *Bull. Korean Chem. Soc*. 29: 463-6.

[26] Mathew, A., Mathew, A., Rao, G. M., and Munichandraiash, N. 2012. "Enhanced Efficiency of Tri-Layered Dye Solar Cells with Hydrothermally Synthesiszedtitania Nanotubes as Light Scattering Outer Layer." *Thin Solid Films* 520: 3581-6.